

# Image Restoration under Significant Additive Noise

Wenyi Zhao<sup>1</sup> and Art Pope

Sarnoff Corporation

201 Washington Road, Princeton, NJ 08540, USA

email: { wzhao, apope }@ieee.org

Tel: 408-523-2178

## Abstract

*The task of deblurring, a form of image restoration, is to recover an image from its blurred version. Whereas most existing methods assume a small amount of additive noise, image restoration under significant additive noise remains an interesting research problem. We describe two techniques to improve the noise handling characteristics of a recently proposed variational framework for semi-blind image deblurring that is based on joint segmentation and deblurring. One technique uses a structure tensor as a robust edge-indicating function. The other uses non-local image averaging to suppress noise. We report promising results with these techniques for the case of a known blur kernel.*

**EDICS**    IMD-ANAL, SAS-ADAP

## I. INTRODUCTION

The task of deblurring, a form of image restoration, is to obtain the original, sharp version of a blurred image. There exist many applications for image restoration [3], including astronomical imaging, medical imaging, law enforcement, and digital media restoration. The problem has attracted strong research interest and will continue to do so, not only because it has many applications but also because it has a simple mathematical formulation yet it is a classical inverse problem [16] for which good solutions are not easily obtained. The simple equation for expressing image blurring/degradation is as follows:

$$g = f * h + n \tag{1}$$

<sup>1</sup> Corresponding Author

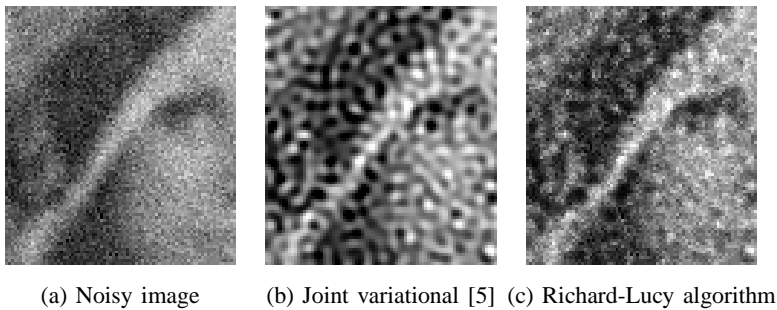


Fig. 1. The effect of significant image noise on image restoration: (a) Noisy blurred image with image intensity in  $[0, 255]$  and additive Gaussian noise of standard deviation 20; (b) Image restored using a joint variational framework [5]; (c) Image restored using the Richard-Lucy algorithm from Matlab. Images in this and other figures are cropped due to page limits.

where  $f$  is the original image and  $g$  is the version that has been degraded through blurring (convolution  $*$ ) by kernel  $h$  and the addition of random noise  $n$ . This degradation model represents a linear relationship between  $f$  and  $g$ ; hence, the problem of recovering  $f$  from  $g$  is called *linear image restoration*. Often the blur kernel is assumed to be space-invariant. If we lack prior knowledge of the blur kernel  $h$ , we have the more difficult *blind (linear) image restoration* problem [13] in which  $h$  also needs to be estimated.

Many algorithms have been proposed to solve this inverse problem [3]: direct Wiener filter methods [2]; iterative methods [11]; variational methods [15], [17]; and blind restoration methods [8], [12], [5]. Without some form of regularization [16], the inverse problem is unstable in the presence of noise, as small fluctuations in noise become amplified into large artifacts in the solution. Regularization is used by most methods to obtain stable solutions, but often the results are less than satisfactory when noise is substantial, as illustrated in (Fig. 1).

This paper addresses the problem of image restoration when additive noise is substantial. We propose to enhance the segmentation step in the joint framework that unifies classical image segmentation and image restoration [5], [12], [9] (Fig. 2). In particular, we implement robust versions of a recently proposed (Fig. 2). In particular, we implement robust versions of a recently proposed variational framework of semi-blind image deblurring [5]. As can be seen from Fig. 2, the basic idea of handling significant image noise is to have a robust image segmentation. Reliable image segmentation (or, equivalently, edge detection) is the key for adaptive image deconvolution where true edges are deblurred while noise is suppressed in other regions.

The remainder of this paper is organized as follows. In Section II, we present the robust variational image restoration framework that handles significant noise. After presenting experimental results in

Section III, we conclude our paper in Section IV.

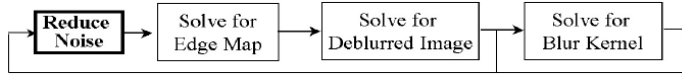


Fig. 2. The variational image restoration process with an additional noise reduction step described here. Solving for the blur kernel is an optional step needed when restoration is blind.

## II. IMAGE RESTORATION UNDER SIGNIFICANT ADDITIVE NOISE

### A. Joint image segmentation and restoration

Image segmentation and restoration are important image processing problems that have been studied extensively. For image segmentation, one popular method is based on the Mumford-Shah functional [14]:

$$\mathcal{F}(f, K) = \frac{1}{2} \int_{\Omega} (f - g)^2 + \beta \int_{\Omega \setminus K} |\nabla f|^2 + \alpha \int_{\Omega} ds \quad (2)$$

where  $\Omega$  represents the whole image region,  $K$  denotes the set of edge pixels,  $\int_{\Omega} ds$  is the total edge length, and  $\Omega \setminus K$  denotes non-edge regions. However, minimizing this functional is difficult because the discontinuity set  $K$  is both discrete and unknown. To circumvent this difficulty, the  $\Gamma$ -convergence framework can be applied [1] where the functional  $\mathcal{F}(f, K)$  is approximated by  $\mathcal{F}_{\epsilon}(f)$ :  $\lim_{\epsilon \rightarrow 0} \mathcal{F}_{\epsilon}(f) = \mathcal{F}(f, K)$ . Representing the discontinuity set by a continuous *edge map* function  $v$  such that  $v(x) \approx 0$  if  $x \in K$ , and  $v(x) \approx 1$  otherwise, yields a more easily solved approximation of the Mumford-Shah functional of the following form [1]:

$$\mathcal{F}_{\epsilon}(f, v) = \frac{1}{2} \int_{\Omega} (f - g)^2 + \beta \int_{\Omega} v^2 |\nabla f|^2 + \alpha [\epsilon |\nabla v|^2 + \int_{\Omega} \frac{1}{4\epsilon} (v - 1)^2] \quad (3)$$

For image restoration, the TV (Total Variational) method is a popular one, employing an L1 smoothing term rather than the more easily solved L2 metric [8], [17]. The functional to be minimized is

$$\mathcal{F}(f, h) = \frac{1}{2} \int_{\Omega} (h * f - g)^2 + \beta \int_{\Omega} |\nabla f|. \quad (4)$$

Note that the segmentation and restoration problems are interdependent: If we can assume to know the correct segmentation of the image, we can then estimate the unknown blur kernel  $h$  based purely on the smoothed profiles of the known edges. Conversely, if we have a good image restoration or deblurring result, we should use it rather than the original blurred image when estimating segmentation. Such observations have led others to propose a joint variational framework that simultaneously addresses both image segmentation and image restoration [12], [5]. By assuming that the unknown blur kernel  $h_{\sigma}$  is

isotropic and Gaussian, authors of [5] have demonstrated successful semi-blind image restoration that is more robust than the total blind image restoration [8] where the kernel form is not restricted.

Coupling the modified Mumford-Shah functional (Eq. 3) with the data term in the restoration functional (Eq. 4), the authors of [5] have proposed the following objective functional:

$$\mathcal{F}_\epsilon(f, v, \sigma) = \frac{1}{2} \int_{\Omega} (h_\sigma * f - g)^2 + G_\epsilon(f, v) + \gamma \int_{\Omega} |\nabla h_\sigma|^2, \quad (5)$$

where the image regularization term  $G_\epsilon$  is defined as

$$G_\epsilon(f, v) = \beta \int_{\Omega} v^2 |\nabla f|^2 + \alpha \int_{\Omega} [\epsilon |\nabla v|^2 + \frac{(v-1)^2}{4\epsilon}]. \quad (6)$$

Note that the last term in Eq. 5 regularizes estimation of the scale of the unknown blur kernel, favoring a large kernel.

### B. Reducing the impact of image noise

Like most existing variational frameworks, this framework (Eq. 5) does not handle significant image noise well (Fig. 1(b)). To understand why, we examine the edge map  $v$  (see Fig. 3), an intermediate product of the framework that, because it represents the segmentation result, is critical to its success. In regions where the edge map indicates edges prevail, deblurring is performed to achieve sharper edges, while elsewhere, smoothing is performed for noise suppression. In the presence of significant noise, edge map estimation (Fig. 3(b)) is seen to break down when compared against the ideal edge map (Fig. 3(c)). The poor edge map estimate derails the restoration process—for example, causing deblurring to be performed in non-edge regions that are misclassified as edge regions. As a result, significant noise is preserved and propagated by the iterative process, creating noticeable restoration artifacts (Fig. 1(b)).

In the remainder of this paper, we describe two methods to stabilize edge map estimation, thus reducing restoration artifacts due to noise. Before doing so, however, we must briefly review the alternate minimization procedure for functional  $\mathcal{F}_\epsilon(f, v, \sigma)$ . The minimization procedure consists of the following steps, which are alternately repeated until certain stopping criteria are met [5]:

- 1) Fixing  $(f, \sigma)$ , solve an Euler-Lagrange equation for  $v$ :

$$2\beta v |\nabla f|^2 + \alpha \left( \frac{v-1}{2\epsilon} \right) - 2\epsilon \alpha \nabla^2 v = 0 \quad (7)$$

- 2) Fixing  $(v, \sigma)$ , solve an Euler-Lagrange equation for image  $f$ :

$$(h_\sigma * f - g) * h_\sigma(-x, -y) - 2\beta \text{Div}(v^2 \nabla f) = 0 \quad (8)$$

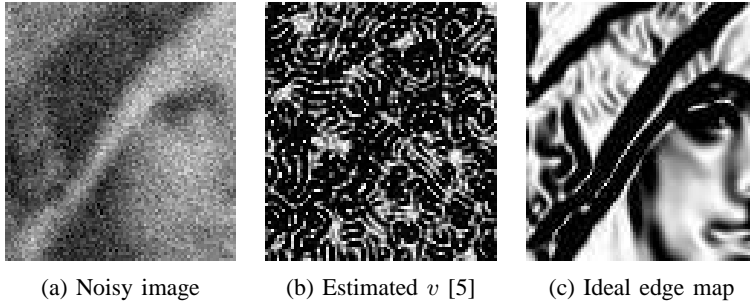


Fig. 3. Edge map ( $v$ ) estimation breaks down with significant noise. The ideal edge map, shown for comparison, was obtained from a blurred but noise-free image. Dark regions are estimated edge pixels.

3) Fixing  $(f, v)$ , solve for the blur kernel scale  $\sigma$ :

$$\int_{\Omega} [(h_{\sigma} * f - g) \left( \frac{\partial h_{\sigma}}{\partial \sigma} * f \right) + \gamma \frac{2h_{\sigma}^2}{\sigma^5} (x^2 + y^2 - 4)(x^2 + y^2)] = 0 \quad (9)$$

Our proposed noise handling methods both seek to improve segmentation by modifying the estimate of  $|\nabla f|^2$  used in Eq. 7. The first method substitutes a new method of computing  $|\nabla f|^2$  itself, while the second substitutes a new estimate of  $f$  into the computation of  $|\nabla f|^2$ .

1) *Structure tensor based robust gradient computation*: Our first noise mitigation method employs the structure tensor commonly used in spatial-temporal optical flow computation and anisotropic diffusion [10]. The pixel-wise structure tensor is used in these methods to determine the geometric type of a pixel. It is defined as

$$S = \begin{pmatrix} f_x^2 & f_x f_y \\ f_y f_x & f_y^2 \end{pmatrix} * h_s, \quad (10)$$

where  $h_s$  is typically a Gaussian filter. Since a true edge pixel has one dominant orientation, eigenanalysis of the  $2 \times 2$  structure tensor can indicate whether or not a pixel is a true edge pixel. A pixel is declared an edge pixel only if its structure tensor satisfies the conditions that the difference between its two eigenvalues is significant and the dominant eigenvalue is large than a pre-defined threshold. Based on this analysis, we can compute an edge-indicating function  $I_S$  ( $I_S = 1$  if edge pixel, and  $I_S = 0$  otherwise) and the computation of  $|\nabla f|^2$  in Eq. 7 is modified as follows:

$$|\nabla f|^2 = I_S (f_x^2 + f_y^2). \quad (11)$$

For better estimation under noisy condition, we compute the image gradients  $f_x$  and  $f_y$  using the following formulae

$$f_x = h_{g,x} * f, \quad f_y = h_{g,y} * f \quad (12)$$

where  $h_{g,x}$  and  $h_{g,y}$  are Gaussian derivative filters.

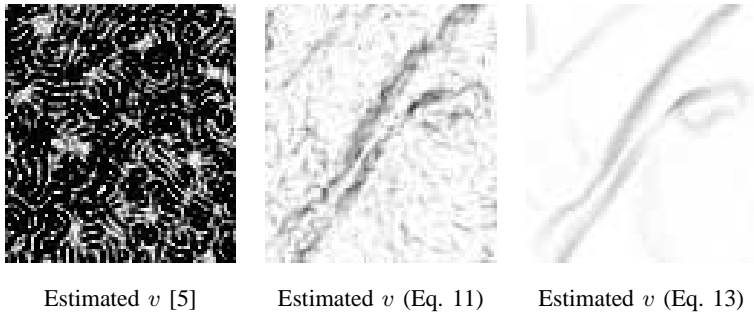


Fig. 4. Improved edge map ( $v$ ) estimation obtained on the noisy image (Fig. 1(a)): (a) the original estimate; (b) improvement using structure tensor alone; (c) improvement using nonlocal image averaging alone.

2) *Nonlocal image averaging*: Our second noise mitigation method modifies the image estimate  $f$  that is obtained from Eq. 8 and used to compute  $|\nabla f|^2$ . The  $|\nabla f|^2$  term in Eq. 7 is replaced by  $|\nabla \tilde{f}|^2$ , where  $\tilde{f}$  is a denoised version of  $f$  obtained using a recently proposed image denoising method, *nonlocal averaging* [6]:

$$\tilde{f}(x, y) = \sum_{(u,v) \in \Omega} w_{(x,y)}(u, v) f(u, v), \quad (13)$$

where the weights  $w_{(x,y)}(u, v)$  depend on the similarity between the pixels  $(x, y)$  and  $(u, v)$ , and satisfy the usual conditions  $0 \leq w_{(x,y)}(u, v) \leq 1$  and  $\sum_{(u,v) \in \Omega} w_{(x,y)}(u, v) = 1$ . As a global method, it is powerful in removing significant noise because it borrows information from all similar pixels across the whole image. The weights  $w_{(x,y)}(u, v)$  are computed as decaying exponential functions centering around  $(x, y)$ :

$$w_{(x,y)}(u, v) = \frac{1}{Z_{(x,y)}(u, v)} e^{-\frac{|N(x,y) - N(u,v)|^2}{d^2}}, \quad (14)$$

where  $N(x, y)$  and  $N(u, v)$  represents neighborhood regions centering around  $(x, y)$  and  $(u, v)$  respectively, and  $d$  controls the decay of the weights as a function of Euclidean distance.  $Z_{(x,y)}(u, v)$  is a normalization factor ensuring that  $\sum_{(u,v) \in \Omega} w_{(x,y)}(u, v) = 1$ .

Fig. 4 illustrates the improved edge map estimation resulting from these techniques. In the following section we show that the improved estimation of  $v$  leads to better image restoration results.

### III. EXPERIMENTAL RESULTS

The performance of the improved variational framework is presented in Fig. 5. The grayscale  $256 \times 256$  pixel Lena image with 256 gray levels is contaminated by additive Gaussian noise with a standard deviation of 20 (plot (a)). In the experiment, we have implemented the following methods and the image restoration results are plotted in Fig. 5 for comparison.

- The original variational framework [5]. Result is shown in plot (b).
- The robust variational framework with the first method of robust gradient computation. The digital Gaussian kernel  $h_s$  in Eq. 10 has a width of 10 and std. dev. of 1. Result is shown in plot (c).
- The robust variational framework with the second method of nonlocal image averaging. The size of the neighborhood regions used for weight computation in Eq. 13 is  $7 \times 7$  pixels. For computational efficiency, the whole image area  $\Omega$  used to search for similar neighborhood regions is reduced to a large region of  $21 \times 21$  centered on the pixel  $(x, y)$ . Restored image is shown in plot (d) and plot (f) is the associated image  $\tilde{f}$  from nonlocal averaging (the unprocessed image border  $(21 - 1)/2 = 10$ ).
- A method based on edge-enhancing anisotropic diffusion [7]. Result is shown in plot (e).

From the comparison, we see the improvements of image restoration under significant noise based on the robust variational framework in terms of edge deblurring and noise suppression. Overall, the robust variational framework based on nonlocal averaging achieves the best result (plot (d)). In terms of pure image denoising, the nonlocal averaging algorithm is the best (plot (f)). However, its computational cost is also much higher (excluding the robust framework that includes it as one component). Finally, the result from anisotropic diffusion is quite good but it provides no true edge deblurring.

#### IV. CONCLUSION

In this paper, we have presented methods to improve existing frameworks of joint segmentation and deblurring to handle significant additive noise. The key idea is to achieve reliable segmentation under significant noise and consequently better image restoration. Two particular methods are presented: structure tensor based robust gradient computation and nonlocal image averaging. A robust variational framework based on these two methods is implemented and tested. Initial results show a clear improvement in restored image quality compared to previous methods. One nice property of the proposed framework is that it works fairly well with images with a small amount of noise too. Elsewhere, other methods have been proposed to handle a different type of image noise [4]: so-called salt-and-pepper noise. It would be interesting to investigate the possibility of designing a comprehensive scheme to handle various types of image noise in image restoration.

#### REFERENCES

- [1] L. Ambrosio and V.M. Tortorelli, "Approximation of Functionals Depending on Jumps by Elliptic Functionals via  $\Gamma$ -Convergence", *Communications on Pure and Applied Mathematics*, Vol. XLIII, pp. 999-1036, 1990.
- [2] H. Andrew and B. Hunt, *Digital Image Restoration*, Englewood Cliffs, NJ:Prentice-Hall, 1977.
- [3] M. Banham and A. Katsaggelos, "Digital Image Restoration", *IEEE Signal Processing Magazine*, 14(2):24-41, 1997.



(a) Noisy Lena image with noise std. dev.=20



(b) Restored image after 4 iterations [5]



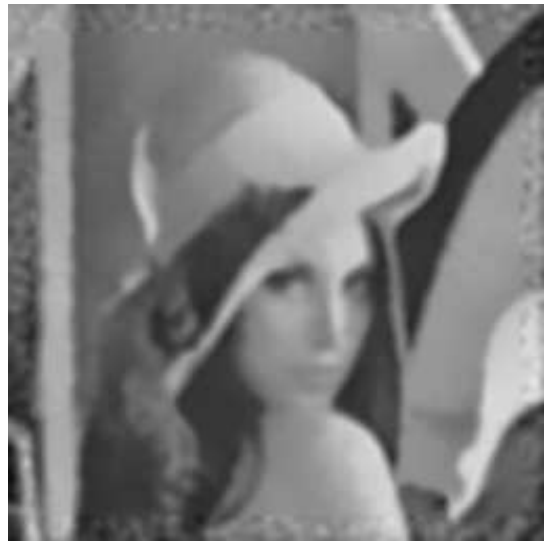
(c) Restored image after 4 iteration: robust gradient



(d) Restored image after 4 iteration: nonlocal averaging



(e) Recovered image: anisotropic diffusion [7]



(f) Nonlocally averaged image after 4 iteration (Eq. 13)

Fig. 5. Comparison of image restoration under significant image noise: (a) Original image (std. dev. = 20), (b) Restored image from the original variational framework, (c) Restored image from the robust framework with robust gradient, (d) Restored image from the robust framework with nonlocal averaging, (e) Recovered image from edge-enhancing anisotropic diffusion. Finally plot (f) is  $\tilde{f}$ , a by-product associated with plot (d).

- [4] L. Bar, N. Sochen, and N. Kiryati, "Image Deblurring in the Presence of Salt-and-Pepper Noise," *Proc. Int. Conf. Scale Space and PDE Methods in Computer Vision*, 2005.
- [5] L. Bar, N. Sochen and N. Kiryati, "Variational Pairing of Image Segmentation and Blind Restoration," *Proc. of European Conference on Computer Vision*, 2004.
- [6] A. Buades, B. Coll, and J. Morel, "A non-local algorithm for image denosing", *Proc. of IEEE Conf. Computer Vision and Pattern Recognition*, 2005.
- [7] M. Black, G. Sapiro, D. Marimont, and D. Heeger, "Robust Anisotropic Diffusion", *IEEE Trans. Image Processing*, Vol. 7, pp. 421-432, 1998.
- [8] T. Chan and C. Wong, "Total Variational Blind Deconvolution", *IEEE Trans. Image Processing*, Vol. 7, pp. 370-375, 1998.
- [9] S. Colonnese, P. Campisi, G. Panci, G. Scarano, "Blind Image Deblurring in the Edge Domain," *Proc. of European Signal Processing Conference*, 2004.
- [10] B. Jahne and H. HauBecker, *Computer Vision and Applications*, Academic Presse, 2000.
- [11] A. Katsaggelos, "Iterative Image Restoration Algorithms", *Optical Engineering*, Vol. 28, pp. 735-748, 1989.
- [12] J. Kim, A. Tsai, M. Cetin, and A. Willsky, "A Curve Evolution-based Variational Approach to Simultaneous Image Restoration and Segmentation", *IEEE Proc. Int. Conf. Image Processing*, Vol.1, pp. 109-112, 2002.
- [13] D. Kundur and D. Hatzinakos, "Blind Image Deconvolution", *Signal Processing Magazine*, Vol. 13, pp. 43-64, 1996.
- [14] D. Mumford and J. Shah, "Optimal Approximations by Piecewise Smooth Functions and Associated Variational Problems", *Communications on Pure and Applied Mathematics*, Vol. 42, pp. 577-684, 1989.
- [15] L. Rudin and S. Osher, "Total Variation Based Image Restoration with Free Local Constraints", *Proc. IEEE Int. Conf. Image Processing*, 1994.
- [16] A. Tikhonov and V. Arsenin, *Solutions of Ill-posed Problems*, New York, 1977.
- [17] C. Vogel and M. Oman, "Fast, Robust Total Variation-based Reconstruction of Noisy, Blurred Images", *IEEE Trans. Image Processing*, Vol. 7, pp. 813-824, 1998.